Requirements on the Spatial Distribution of Elastic Components Used in Compliance Realization

Shuguang Huang and Joseph M. Schimmels

Abstract— **In this paper, necessary conditions on the locations and orientations of elastic components in a compliant mechanism used to realize any given spatial compliance are identified. The topologies considered are either fully parallel or fully serial mechanisms having an arbitrary number of lumped elastic components. It is shown that the requirements on elastic components are characterized by a sphere for the location distribution and by three cones for the orientation distribution. The easy to assess conditions on the set of components can be used to achieve a more desirable mechanism geometry when used in conjunction with existing spatial compliance synthesis procedures.**

Keywords: compliant joints and mechanisms, mechanical design, spatial stiffness and compliance, compliance realization

I. Introduction

In robotic manipulation, some form of compliance is needed to improve the accuracy of constrained relative positioning and to provide force regulation [1], [2]. Stable constrained manipulation can be obtained by a passive elastic suspension of the end-effector. If small deflection is considered, a compliance is described by a linear mapping between the force applied to the object and the resulting relative motion of the object. For the spatial case, the relationship can be expressed as [3]:

$$\mathbf{w} = \mathbf{K}\mathbf{t}, \quad \text{or} \quad \mathbf{t} = \mathbf{C}\mathbf{w}, \tag{1}$$

where $\mathbf{w} \in \mathbb{R}^6$ is the applied wrench (force and moment), $\mathbf{t} \in \mathbb{R}^6$ is the motion twist (translation and rotation) of the object, and where $\mathbf{K} \in \mathbb{R}^{6\times6}$ and $\mathbf{C} \in \mathbb{R}^{6\times6}$ are the stiffness matrix and compliance matrix, respectively. If the wrench $\mathbf{w}$ and twist $\mathbf{t}$ are described in Plücker's ray and axis coordinates (or vice versa) respectively, both $\mathbf{K}$ and $\mathbf{C}$ are symmetric positive semidefinite (PSD).

Many researchers have investigated general spatial compliant behaviors. In spatial compliance analysis, screw theory [3]–[6] and Lie groups [7], [8] have been used. In prior work on compliance realization, compliant mechanisms are designed to attain a given elastic behavior. Most early synthesis procedures for fully parallel and fully serial mechanisms were based on an algebraic decomposition of the stiffness/compliance matrix [9]–[16]. Others addressed the analysis, modeling and synthesis of compliance associated with mechanisms composed of distributed elastic components [17]–[21].

This research was supported by the National Science Foundation under Grant CMMI-2024554. Shuguang Huang and Joseph M. Schimmels are with the Department of Mechanical Engineering, Marquette University, Milwaukee, WI 53201-1881 USA (e-mail: huangs@marquette.edu; j.schimmels@marquette.edu).

In [22], geometric construction based synthesis procedures were developed for general spatial elastic properties realized using either fully parallel or fully serial mechanisms having lumped elastic components, and the concept of dual elastic mechanisms in parallel and serial construction was introduced. A parallel mechanism and a serial mechanism at given configurations are elastic duals if they are capable of achieving the exact same space of compliant behaviors when the mechanisms have infinite variation in spring stiffness and joint compliance. In [23], the concept of dual elastic mechanisms was extended to rank-deficient cases.

Although geometric construction-based synthesis procedures to realize a given spatial compliance with the minimum number of elastic components have been already identified [22], general guidance for the overall design in the early stages of the process is needed. In the synthesis process, the allowable space of remaining components depends on the previously selected elastic components. Guidance to judiciously select the elastic components in the first one or two steps to ensure the obtained mechanism has desirable geometry is an important issue. In [24], elastic component distribution relative to the stiffness center and compliance center was identified. However, the requirements on the distribution in location and direction of elastic components were not identified.

This paper addresses the distribution conditions on mechanisms used to realize an arbitrary compliance. The topologies considered are either fully parallel or fully serial mechanisms having an arbitrary number of elastic components. Each mechanism is composed of rigid links connected by lumped elastic components. The physical implications of these conditions are provided.

The paper is outlined as follows. Section II provides the technical context needed for the development of the distribution theory. In Section III, a set of necessary conditions on the elastic component distribution is presented both for parallel and for serial mechanisms. In Section IV, an extremal property associated with the distribution theory is identified. In Section V, discussion on the physical significance and application of the distribution theory is provided. A brief summary appears in Section VI.

II. Background

In compliance realization, fully parallel mechanisms and fully serial mechanisms have the simplest topology. In this section, screw descriptions of the geometry of these two types of mechanisms and their use in the realization of spatial compliance are reviewed. To realize a full-rank elastic behavior, the number of elastic components in a mechanism must be no less than 6.

A. Parallel Mechanisms

Consider a parallel mechanism with $m \geq 6$ springs. To realize a general stiffness matrix $\mathbf{K}$, *screw springs* (springs that provide force along and torque about in the same axis) must be used [11]. The geometry of each spring i is described by a unit screw wrench $\mathbf{w}_i$ defined as the *spring wrench* having the form:

$$\mathbf{w}_i = \left[\begin{array}{c} \mathbf{n}_i \\ p_i\mathbf{n}_i + \mathbf{r}_i \times \mathbf{n}_i \end{array} \right], \tag{2}$$

where $\mathbf{n}_i$ is a unit 3-vector indicating the direction of the spring i axis, p_i is the pitch of the screw, and $\mathbf{r}_i$ is the minimum-length vector from the coordinate origin (perpendicular) to the spring axis. If $k_i > 0$ is the spring rate associated with $\mathbf{w}_i$, the Cartesian stiffness associated with the m-spring mechanism is [11]:

$$\mathbf{K} = k_1\mathbf{w}_1\mathbf{w}_1^T + k_2\mathbf{w}_2\mathbf{w}_2^T + \cdots + k_n\mathbf{w}_m\mathbf{w}_m^T. \tag{3}$$

Conversely, if a Cartesian stiffness matrix in the partitioned form

$$\mathbf{K} = \left[\begin{array}{cc} \mathbf{A} & \mathbf{B} \\ \mathbf{B}^T & \mathbf{D} \end{array} \right] \tag{4}$$

is decomposed into the form of (3), the stiffness is realized with a parallel mechanism having m springs described by spring wrenches $\mathbf{w}_i$s.

If the pitch $p_i = 0$ in (2), then $\mathbf{w}_i$ represents a conventional line spring. As shown in [9], a full-rank stiffness $\mathbf{K}$ can be realized with a set of simple springs (conventional line springs and torsional springs) if and only if the off-diagonal block of (4) satisfies

$$\text{trace}(\mathbf{B}) = 0. \tag{5}$$

B. Serial Mechanisms

The duality between parallel mechanisms used for stiffness realization and serial mechanisms used for compliance realization was identified in [14] and was used in the synthesis of compliant behaviors with serial mechanisms [25], [26]. As shown in [14], in the realization of a general compliance with a serial mechanism, helical joints must be used. The geometry of each joint i is described by a unit screw twist $\mathbf{t}_i$ defined as the *joint twist* having the form:

$$\mathbf{t}_i = \left[\begin{array}{c} p_i\mathbf{n}_i + \mathbf{r}_i \times \mathbf{n}_i \\ \mathbf{n}_i \end{array} \right], \tag{6}$$

where $\mathbf{n}_i$ is a unit 3-vector indicating the direction of the joint i rotation axis, p_i is the pitch of the helical joint, and $\mathbf{r}_i$ is the perpendicular vector from the coordinate origin to the twist axis. If $c_i > 0$ is the joint compliance associated with $\mathbf{t}_i$, the Cartesian compliance matrix associated with the m-joint mechanism is [14]:

$$\mathbf{C} = c_1\mathbf{t}_1\mathbf{t}_1^T + c_2\mathbf{t}_2\mathbf{t}_2^T + \cdots + c_n\mathbf{t}_m\mathbf{t}_m^T. \tag{7}$$

Conversely, if a compliance matrix in the partitioned form

$$\mathbf{C} = \left[\begin{array}{cc} \mathbf{G} & \mathbf{H} \\ \mathbf{H}^T & \mathbf{Q} \end{array} \right] \tag{8}$$

is decomposed into the form of (7), the compliance matrix is realized with a serial mechanism having m joints described by joint twists $\mathbf{t}_i$s.

If the pitch $p_i = 0$ in (6), then $\mathbf{t}_i$ represents a conventional revolute joint. As shown in [27], a full-rank compliance matrix $\mathbf{C}$ can be realized with a serial mechanism having conventional revolute and prismatic joints if and only if the off-diagonal block of (8) satisfies

$$\text{trace}(\mathbf{H}) = 0. \tag{9}$$

In this paper, the realization of a desired elastic behavior with either a fully parallel or a fully serial mechanism is considered. In each case, the elastic behavior is readily described by the screws associated with its elastic primitives, either as spring wrenches (3) or joint twists (7). Below, we show that a given elastic behavior imposes conditions on the spatial distribution of the mechanism screws.

III. Elastic Component Distribution in a Mechanism

In this section, elastic component distribution conditions for a parallel mechanism and for a serial mechanism are developed. First, the distribution conditions on spring locations and orientations in a parallel mechanism are derived. Then, by duality, the distribution conditions on joint axis locations and orientations in a serial mechanism are obtained.

A. Parallel Mechanisms

In the following, distribution conditions on spring *locations* are first derived. Then, distribution conditions on spring *directions* are developed.

In [24], the distribution of springs relative to the stiffness center was addressed. It was shown that, to realize a given stiffness matrix with a parallel mechanism, the springs must surround the stiffness center. Specifically, it was shown that the stiffness weighted average distance from the stiffness center to the spring axes is zero. The conditions on the distribution of spring locations and directions derived below are more restrictive and are independent from that presented in [24].

1) Spring Location Distribution: Consider a parallel mechanism with spring wrenches described in an arbitrary coordinate frame as $(\mathbf{w}_1, \mathbf{w}_2, ..., \mathbf{w}_m)$, where each wrench has the form of (2). If k_i is the spring rate associated with $\mathbf{w}_i$, the rank-1 stiffness matrix associated with a single spring is:

$$\mathbf{K}_i = k_i\mathbf{w}_i\mathbf{w}_i^T = \left[\begin{array}{cc} \mathbf{A}_i & \mathbf{B}_i \\ \mathbf{B}_i^T & \mathbf{D}_i \end{array} \right], \tag{10}$$

where

$$\begin{aligned} \mathbf{A}_i &= k_i\mathbf{n}_i\mathbf{n}_i^T, & (11) \\ \mathbf{B}_i &= k_i\left[p_i\mathbf{n}_i\mathbf{n}_i^T + \mathbf{n}_i(\mathbf{r}_i \times \mathbf{n}_i)^T\right], & (12) \\ \mathbf{D}_i &= k_i(p_i\mathbf{n}_i + \mathbf{r}_i \times \mathbf{n}_i)(p_i\mathbf{n}_i + \mathbf{r}_i \times \mathbf{n}_i)^T. & (13) \end{aligned}$$

The stiffness matrix $\mathbf{K}$ realized with the m-spring mechanism is:

$$\mathbf{K} = \sum_{i=1}^{m} k_i \mathbf{w}_i \mathbf{w}_i^T = \sum_{i=1}^{m} \mathbf{K}_i. \tag{14}$$

If $\mathbf{K}$ is partitioned in the form of (4), then

$$\mathbf{A} \;=\; \sum_{i=1}^{m} k_i \mathbf{n}_i \mathbf{n}_i^T, \tag{15}$$

and

$$\mathbf{D} \;=\; \sum_{i=1}^{m} k_i (p_i \mathbf{n}_i + \mathbf{r}_i \times \mathbf{n}_i)(p_i \mathbf{n}_i + \mathbf{r}_i \times \mathbf{n}_i)^T. \tag{16}$$

Expanding (16) yields:

$$\mathbf{D} = \sum_{i=1}^{m} k_i [p_i^2 \mathbf{n}_i \mathbf{n}_i^T + p_i (\mathbf{r}_i \times \mathbf{n}_i)\mathbf{n}_i^T + p_i \mathbf{n}_i (\mathbf{r}_i \times \mathbf{n}_i)^T + (\mathbf{r}_i \times \mathbf{n}_i)(\mathbf{r}_i \times \mathbf{n}_i)^T]. \tag{17}$$

Denote

$$\mathbf{u}_i = \mathbf{r}_i \times \mathbf{n}_i, \quad i = 1, 2, ..., m, \tag{18}$$

then the 3×3 block matrix $\mathbf{D}$ in (4) is expressed as:

$$\mathbf{D} = \sum_{i=1}^{m} k_i \left[p_i^2 \mathbf{n}_i \mathbf{n}_i^T + p_i \mathbf{u}_i \mathbf{n}_i^T + p_i \mathbf{n}_i \mathbf{u}_i^T + \mathbf{u}_i \mathbf{u}_i^T \right]. \tag{19}$$

Since $\mathbf{n}_i$ is a unit 3-vector and $\mathbf{n}_i \perp \mathbf{r}_i$,

$$\|\mathbf{u}_i\| \;=\; \|\mathbf{r}_i \times \mathbf{n}_i\| = \|\mathbf{r}_i\|, \tag{20}$$
$$\mathbf{u}_i^T \mathbf{u}_i \;=\; \mathbf{r}_i^T \mathbf{r}_i, \tag{21}$$
$$\text{trace}(\mathbf{n}_i \mathbf{n}_i^T) \;=\; \mathbf{n}_i^T \mathbf{n}_i = 1, \tag{22}$$
$$\text{trace}(\mathbf{n}_i \mathbf{u}_i^T) \;=\; \text{trace}(\mathbf{u}_i \mathbf{n}_i^T) = \mathbf{u}_i^T \mathbf{n}_i = 0. \tag{23}$$

Thus,

$$\begin{aligned} \text{trace}(\mathbf{D}) &= \sum_{i=1}^{m} k_i \text{trace}\big(p_i^2 \mathbf{n}_i \mathbf{n}_i^T + p_i \mathbf{u}_i \mathbf{n}_i^T + p_i \mathbf{n}_i \mathbf{u}_i^T + \mathbf{u}_i \mathbf{u}_i^T\big) \\ &= \sum_{i=1}^{m} k_i \left[p_i^2 \text{trace}(\mathbf{n}_i \mathbf{n}_i^T) + \text{trace}(\mathbf{u}_i \mathbf{u}_i^T) \right] \\ &= \sum_{i=1}^{m} k_i \left(p_i^2 + r_i^2 \right), \end{aligned} \tag{24}$$

where $r_i = \|\mathbf{r}_i\| = \|\mathbf{u}_i\|$ is the perpendicular distance from the origin to spring wrench $\mathbf{w}_i$. If we denote

$$d_i = \sqrt{r_i^2 + p_i^2}, \quad i = 1, 2, ..., m, \tag{25}$$

then, (24) can be written as

$$\text{trace}(\mathbf{D}) = k_1 d_1^2 + k_2 d_2^2 + \cdots + k_m d_m^2. \tag{26}$$

For a given $\mathbf{K}$ realized by a specific m-spring mechanism, denote

$$d_{\max} \;=\; \max\{d_1, d_2, ..., d_m\}, \tag{27}$$
$$d_{\min} \;=\; \min\{d_1, d_2, ..., d_m\}, \tag{28}$$

then,

$$\left(\sum_{i=1}^{m} k_i \right) d_{\min}^2 \;\le\; \text{trace}(\mathbf{D}) \;\le\; \left(\sum_{i=1}^{m} k_i \right) d_{\max}^2. \tag{29}$$

Since [from (15) and (22)]

$$\sum_{i=1}^{m} k_i = \text{trace}(\mathbf{A}), \tag{30}$$

inequality (29) can be expressed as:

$$d_{\min} \;\le\; \sqrt{\frac{\text{trace}(\mathbf{D})}{\text{trace}(\mathbf{A})}} \;\le\; d_{\max}. \tag{31}$$

Denote

$$\rho_k = \sqrt{\frac{\text{trace}(\mathbf{D})}{\text{trace}(\mathbf{A})}} \tag{32}$$

as the radius of a sphere S_k centered at the coordinate frame:

$$x^2 + y^2 + z^2 = \rho_k^2. \tag{33}$$

Then, inequality (29) becomes

$$d_{\min} \;\le\; \rho_k \;\le\; d_{\max}. \tag{34}$$

Since ρ_k is effectively the stiffness weighted average distance d_i from the origin, the equality holds in (34) if and only if $d_{\min} = d_{\max}$, which means all d_is in (26) have the same value. Thus, in the generic case,

$$d_{\min} \;<\; \rho_k \;<\; d_{\max}. \tag{35}$$

Let P_i be the point on the axis of the ith spring wrench $\mathbf{w}_i$ associated with the perpendicular position vector $\mathbf{r}_i$, and T_i be the point on the axis of $\mathbf{w}_i$ determined by $|P_i T_i| = |p_i|$ as shown in Fig. 1 for $i = \alpha, \beta$, then the position vector of T_i in a coordinate frame at O is:

$$\mathbf{d}_i = \mathbf{r}_i + p_i \mathbf{n}_i, \quad i = 1, 2, ..., m. \tag{36}$$

It can be seen that vector $\mathbf{d}_i$ has the length d_i defined in (25). Consider the vector $\mathbf{d}_\alpha$ defined in (36) that has the maximum length $d_{\max} = \|\mathbf{d}_\alpha\|$, then by inequality (35), $d_\alpha > \rho_k$, which means the distance to point T_α from the origin is greater than the radius of sphere S_k (the average distance from the origin). Thus, T_α must be outside the sphere as illustrated in Fig. 1.

Similar reasoning applies to the point T_β that has minimum distance $d_{\min}$ from the origin. Inequality (35) requires that T_β is inside sphere S_k.

2) Spring Direction Distribution: Now consider the symmetric 3×3 block matrix $\mathbf{A}$ in (4). The three eigenvalues k_i and the corresponding eigenvectors (in the direction of the wrench-compliant axes [6]) are invariant. In a coordinate frame aligned with the wrench-compliant axes, matrix $\mathbf{A}$ has diagonal form:

$$\mathbf{A}_\lambda = \text{diag}(\lambda_1, \lambda_2, \lambda_3). \tag{37}$$

Suppose in the same coordinate frame the direction unit vectors $\mathbf{n}_j$ for each spring j are:

$$\mathbf{n}_j = [n_{j1}, n_{j2}, n_{j3}]^T, \quad j = 1, 2, ..., m. \tag{38}$$

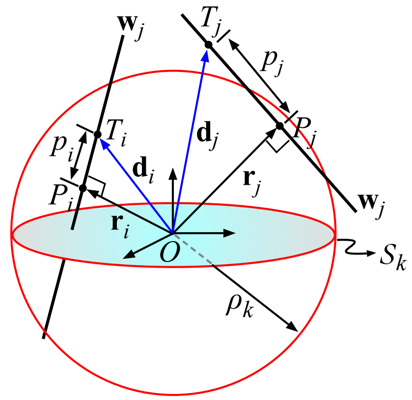

Fig. 1. Distribution of spring locations. At least one T_i (T_α) must be outside sphere S_k and at least one T_j (T_β) must be inside sphere S_k.

By (15) and (38), along each eigenvector i,

$$\lambda_i = k_1 n_{1i}^2 + k_2 n_{2i}^2 + ... + k_m n_{mi}^2, \quad i = 1, 2, 3. \tag{39}$$

For $i = 1, 2, 3$, denote

$$n_{i,\max} = \max\{|n_{1i}|, |n_{2i}|, ..., |n_{mi}|\}, \tag{40}$$
$$n_{i,\min} = \min\{|n_{1i}|, |n_{2i}|, ..., |n_{mi}|\}, \tag{41}$$

then,

$$\left(\sum_{j=1}^{m} k_j\right) n_{i,\min}^2 \leq \lambda_i \leq \left(\sum_{j=1}^{m} k_j\right) n_{i,\max}^2. \tag{42}$$

Since

$$\sum_{j=1}^{m} k_j = \text{trace}(\mathbf{A}_\lambda) = \sum_{i=1}^{3} \lambda_i = \text{trace}(\mathbf{A}), \tag{43}$$

$$n_{i,\min} \leq \sqrt{\frac{\lambda_i}{\text{trace}(\mathbf{A})}} \leq n_{i,\max}. \tag{44}$$

Denote

$$\eta_i = \sqrt{\frac{\lambda_i}{\text{trace}(\mathbf{A})}}, \quad i = 1, 2, 3, \tag{45}$$

which is effectively the stiffness weighted average orientation of the spring wrenches with respect to the i direction. Then the angle defined by

$$\theta_i = \cos^{-1} \eta_i \tag{46}$$

indicates the stiffness weighted average angle of the spring axes with respect to the i-axis ($i = 1, 2, 3$).

Let θ_{ji} ($0 \leq \theta_{ji} \leq \pi/2$) be the angle between $\mathbf{n}_j$ and the i-axis, then,

$$|n_{ji}| = \cos\theta_{ji}, \quad j = 1, 2, ..., m; \; i = 1, 2, 3. \tag{47}$$

Thus, $n_{i,\min}$ and $n_{i,\max}$ correspond to the 2 direction vectors that have the largest and smallest angles with respect to the ith axis, $\theta_{i,\max}$ and $\theta_{i,\min}$, i.e.,

$$n_{i,\min} = \cos\theta_{i,\max}, \quad n_{i,\max} = \cos\theta_{i,\min}. \tag{48}$$

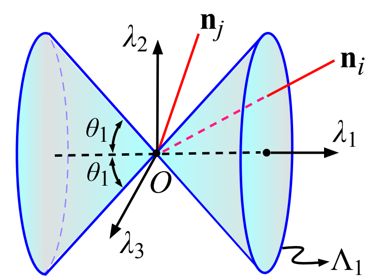

Fig. 2. Spring direction distribution constrained by cone Λ_1. Among all the direction vectors, at least one direction vector ($\mathbf{n}_\xi$) must be outside cone Λ_1 and at least one direction vector ($\mathbf{n}_\nu$) must be inside cone Λ_1.

Inequality (44) requires:

$$\theta_{i,\min} \leq \theta_i \leq \theta_{i,\max}, \quad i = 1, 2, 3. \tag{49}$$

The equality holds if and only if $\theta_{i,\min} = \theta_{i,\max}$, which means all spring wrench axes have the same angle with respect to the ith axis. Thus, in the generic case,

$$\theta_{i,\min} < \theta_i < \theta_{i,\max}, \quad i = 1, 2, 3. \tag{50}$$

The physical meaning of this condition can be represented geometrically by the following.

In a coordinate frame along the wrench-compliant axes, let Λ_i be the cone formed by lines that pass through the origin and have angle θ_i in (46) with respect to the axis associated with eigenvalue λ_i. There are 3 cones Λ_1, Λ_2 and Λ_3 symmetric about the 3 coordinate axes (in the directions of wrench-compliant axes), respectively. Consider the direction vector $\mathbf{n}_\xi$ that has the maximum angle $\theta_{i,\max}$ with respect to axis i. By inequality (50), the angle must be greater than the angle θ_i between the edges of cone Λ_i and the ith axis. Thus, $\mathbf{n}_\xi$ must be outside cone Λ_i. Similar reasoning applies to direction vector $\mathbf{n}_\nu$ that has the minimum angle with respect to the ith axis. Thus, $\mathbf{n}_\nu$ must be inside cone Λ_i.

Therefore, among all direction vectors, at least one must be inside cone Λ_i and at least one must be outside cone Λ_i. Figure 2 illustrates the direction distribution condition associated with cone Λ_1. The same condition holds for the other two cones Λ_2 and Λ_3.

Since

$$\cos^2\theta_1 + \cos^2\theta_2 + \cos^2\theta_3 = \sum_{i=1}^{3} \frac{\lambda_i}{\text{trace}(\mathbf{A})} = 1, \tag{51}$$

$\cos^2\theta_i + \cos^2\theta_j < 1$ for $i \neq j$. Hence,

$$\theta_1 + \theta_2 > \frac{\pi}{2}, \quad \theta_1 + \theta_3 > \frac{\pi}{2}, \quad \theta_2 + \theta_3 > \frac{\pi}{2}. \tag{52}$$

Thus, every two cones of Λ_1, Λ_2 and Λ_3 intersect at an infinite number of points, and

$$\mathbb{R}^3 = \Lambda_1 \cup \Lambda_2 \cup \Lambda_3. \tag{53}$$

Thus, any direction vector $\mathbf{n}$ must lie in one of these 3 cones.

In summary, for a parallel mechanism used to realize a given stiffness matrix $\mathbf{K}$, we have:

PROPOSITION 1. If a given stiffness matrix is realized with a parallel mechanism, then,

(i) At least one point T_i (at the end of vector $\mathbf{d}_i$) must be outside sphere S_k (T_α in Fig. 1) and at least one point must be inside the sphere (T_β);

(ii) For each cone Λ_i defined by angle θ_i in (46), at least one spring direction $\mathbf{n}_j$ must be outside Λ_i ($\mathbf{n}_\xi$ in Fig. 2) and at least one spring direction must be inside Λ_i ($\mathbf{n}_\nu$).

B. Serial Mechanisms

As shown in [24], to realize a given compliance matrix with a serial mechanism, the joint axes must surround the compliance center. The conditions identified below further restrict the distributions of joint locations and axes and are independent from that presented in [24].

By duality, the spring distribution conditions for parallel mechanisms in the realization of stiffness can be modified for serial mechanisms in the realization of compliance.

Suppose a serial mechanism has joint twists $\mathbf{t}_i$ in the form of (6) and a compliance matrix $\mathbf{C}$ in (8) is realized with the serial mechanism. Then, a sphere S_c with radius ρ_c is defined by:

$$x^2 + y^2 + z^2 = \rho_c^2, \tag{54}$$

where

$$\rho_c = \sqrt{\frac{\text{trace}(\mathbf{G})}{\text{trace}(\mathbf{Q})}}. \tag{55}$$

If γ_1, γ_2 and γ_3 are the three eigenvalues of $\mathbf{Q}$, similar to (46), three angles are determined by:

$$\phi_i = \cos^{-1}\left(\sqrt{\frac{\gamma_i}{\text{trace}(\mathbf{Q})}}\right), \quad i = 1, 2, 3. \tag{56}$$

Three cones Φ_i ($i = 1, 2, 3$) having angles ϕ_i with respect to the coordinate axes aligned with the twist-compliant axes [6] are defined. Similar to Proposition 1 for parallel mechanisms and with an equivalent definition of vectors $\mathbf{d}_i$ and T_i in (36) for joint twists of (6), we have:

PROPOSITION 2. If a given compliance matrix is realized with a serial mechanism, then,

(i) At least one point T_i (at the end of $\mathbf{d}_i$) must be outside sphere S_c and at least one point must be inside the sphere;

(ii) For each cone Φ_i defined by angle ϕ_i in (56), at least one joint axis direction $\mathbf{n}_j$ must be outside Φ_i and at least one joint axis direction must be inside the cone.

IV. MINIMUM RADIUS OF THE RESTRICTIVE SPHERES

Note the spring distribution requirements hold for an arbitrary coordinate frame. It is known that the trace of the block matrix $\mathbf{A}$ is invariant to coordinate transformation, but the trace of the block matrix $\mathbf{D}$ is not. Thus, in different coordinate frames, the center of sphere S_k is always located at the frame origin, but the radius of the sphere, ρ_k, depends on the coordinate frame selected. Below, it is proved that ρ_k has a minimum value when the coordinate frame is located at the center of stiffness.

The center of stiffness is the location where the stiffness matrix has a symmetric off-diagonal block [7]. Thus, at the stiffness center, the stiffness matrix $\mathbf{K}_c$ has the form:

$$\mathbf{K}_c = \begin{bmatrix} \mathbf{A}_c & \mathbf{B}_c \\ \mathbf{B}_c & \mathbf{D}_c \end{bmatrix}. \tag{57}$$

Then, by definition (32), the radius of the restrictive sphere S_k^c centered at the stiffness center is:

$$\rho_k^c = \sqrt{\frac{\text{trace}(\mathbf{D}_c)}{\text{trace}(\mathbf{A}_c)}}. \tag{58}$$

Let $\tilde{\mathbf{K}}$ be the stiffness matrix describing the same elastic behavior expressed in a coordinate frame at an arbitrary location $\tilde{O}$ having the form:

$$\tilde{\mathbf{K}} = \begin{bmatrix} \tilde{\mathbf{A}} & \tilde{\mathbf{B}} \\ \tilde{\mathbf{B}}^T & \tilde{\mathbf{D}} \end{bmatrix}. \tag{59}$$

The radius of the restrictive sphere $\tilde{S}_k$ centered at this location is:

$$\tilde{\rho}_k = \sqrt{\frac{\text{trace}(\tilde{\mathbf{D}})}{\text{trace}(\tilde{\mathbf{A}})}}. \tag{60}$$

Below we prove that $\rho_k^c \leq \tilde{\rho}_k$.

Since a rotational transformation does not change the trace of any block matrix in (57), only translational transformations of $\mathbf{K}_c$ are considered. Let $\mathbf{T}$ be the translational transformation from the stiffness center to the location $\tilde{O}$:

$$\mathbf{T} = \begin{bmatrix} \mathbf{I} & \mathbf{0} \\ \mathbf{P} & \mathbf{I} \end{bmatrix}, \tag{61}$$

where $\mathbf{I}$ is the 3×3 identity matrix and $\mathbf{P}$ is the 3×3 skew symmetric matrix associated with the translation. Then,

$$\begin{aligned} \tilde{\mathbf{K}} = \begin{bmatrix} \tilde{\mathbf{A}} & \tilde{\mathbf{B}} \\ \tilde{\mathbf{B}}^T & \tilde{\mathbf{D}} \end{bmatrix} &= \mathbf{T}\mathbf{K}_c\mathbf{T}^T \\ &= \begin{bmatrix} \mathbf{I} & \mathbf{0} \\ \mathbf{P} & \mathbf{I} \end{bmatrix} \begin{bmatrix} \mathbf{A}_c & \mathbf{B}_c \\ \mathbf{B}_c & \mathbf{D}_c \end{bmatrix} \begin{bmatrix} \mathbf{I} & \mathbf{P}^T \\ \mathbf{0} & \mathbf{I} \end{bmatrix} \\ &= \begin{bmatrix} \mathbf{A}_c & \mathbf{A}_c\mathbf{P}^T + \mathbf{B}_c \\ \mathbf{P}\mathbf{A}_c + \mathbf{B}_c & \mathbf{P}\mathbf{A}_c\mathbf{P}^T + \mathbf{B}_c\mathbf{P}^T + \mathbf{P}\mathbf{B}_c + \mathbf{D}_c \end{bmatrix} \end{aligned} \tag{62}$$

The lower diagonal 3×3 block in $\tilde{\mathbf{K}}$ is:

$$\tilde{\mathbf{D}} = \mathbf{P}\mathbf{A}_c\mathbf{P}^T + \mathbf{B}_c\mathbf{P}^T + \mathbf{P}\mathbf{B}_c + \mathbf{D}_c. \tag{63}$$

Since $\mathbf{B}_c$ is symmetric and $\mathbf{P}$ is skew-symmetric,

$$\text{trace}(\mathbf{P}\mathbf{B}_c) = \text{trace}(\mathbf{B}_c\mathbf{P}^T) = 0. \tag{64}$$

Thus,

$$\begin{aligned} \text{trace}(\tilde{\mathbf{D}}) &= \text{trace}\left(\mathbf{P}\mathbf{A}_c\mathbf{P}^T + \mathbf{B}_c\mathbf{P}^T + \mathbf{P}\mathbf{B}_c + \mathbf{D}_c\right) \\ &= \text{trace}(\mathbf{P}\mathbf{A}_c\mathbf{P}^T) + \text{trace}(\mathbf{D}_c). \end{aligned} \tag{65}$$

Since $\mathbf{A}_c$ is positive definite, by Sylvester's law of inertia, $\mathbf{P}\mathbf{A}_c\mathbf{P}^T$ must be positive semidefinite. Hence,

$$\text{trace}(\mathbf{P}\mathbf{A}_c\mathbf{P}^T) \geq 0, \tag{66}$$

and the equality holds if and only if $\mathbf{P} = \mathbf{0}$. Therefore,

$$\text{trace}(\tilde{\mathbf{D}}) \ \geq \ \text{trace}(\mathbf{D}_c) \tag{67}$$

for all translational transformations. The equality holds if and only if the coordinate frame is located at the center of stiffness. This proves that the trace of the 3×3 lower diagonal block in the stiffness matrix takes the minimum value at the stiffness center.

Since the trace of $\mathbf{A}_c$ is invariant for coordinate transformations, trace$(\mathbf{A}_c)$ = trace$(\tilde{\mathbf{A}})$. Comparing (58) and (60), we have:

$$\rho_k^c \ \leq \ \tilde{\rho}_k, \tag{68}$$

which proves that the radius of sphere S_k has the minimum value at the center of stiffness.

Similarly, the radius ρ_c of sphere S_c defined in (55) has the minimum value at the center of compliance.

V. Discussion

In this section, the significance of the distribution conditions on the design of a compliant mechanism is addressed. The applications of the results to the special case of zero pitch screws and the special case of planar mechanisms are also presented. Use of these conditions in elastic behavior synthesis procedures is also described.

A. Significance of the Distribution Conditions

In a stiffness matrix $\mathbf{K}$ as partitioned in (4), the trace of $\mathbf{A}$ indicates the overall stiffness in translation and the trace of $\mathbf{D}$ indicates the overall stiffness in rotation. The parameter ρ_k in (32) indicates the amount of moment generated relative to the amount of force generated by the springs of a parallel mechanism. If condition (i) of Proposition 1 is violated, the force from the mechanism is either excessive or insufficient relative to the moment required for the compliant behavior.

Since the moment depends on the coordinate frame used to describe the elastic behavior, ρ_k has different values in different coordinate frames. As proved in Section IV, ρ_k takes its minimum value at the center of stiffness, which indicates that at the stiffness center the translational and rotational aspects of the stiffness are maximally decoupled as stated in [7]. Since the sphere S_k has the minimum radius at the stiffness center, the lower bound of condition (i) of Proposition 1 is most restrictive when the behavior is described at the center of stiffness. Thus, in general this condition should be evaluated at the stiffness center.

The three cones defined in Section III-B are about the three coordinate axes directed along the wrench-compliant axes which constrain the distribution of the spring axis directions. If, in a parallel mechanism, no spring axis direction is in one cone, the mechanism is not able to provide sufficient stiffness along the corresponding wrench-compliant axis, and thus cannot realize the given behavior.

The significance of the distribution conditions in Proposition 2 for serial mechanisms can be similarly interpreted in terms of the compliance matrix and motions in translation and rotation.

B. Mechanisms with Simple Elastic Components

If, for a given stiffness matrix, the trace of $\mathbf{B}$ is zero [satisfies (5)], the stiffness matrix can be realized with a set of line springs (i.e., springs associated with wrenches of zero pitch). Since $p_i = 0$, the position vector $\mathbf{d}_i$ defined in (36) is only the position vector $\mathbf{r}_i$ to the spring axis. Thus, Proposition 1(i) becomes: among all springs in the parallel mechanism, at least one must intersect sphere S_k of radius ρ_k defined in (32) centered at the origin of the coordinate frame; and at least one must not intersect the sphere.

As an application of the distribution theory, consider an object and a desired stiffness matrix $\mathbf{K}$. If the object is inside the sphere S_k determined by (32), then the stiffness matrix cannot be achieved by any simple parallel mechanism ($p_i = 0$, $i = 1, 2, ..., m$) regardless of the number of springs and values of spring rates even if $\mathbf{K}$ satisfies (5). This is because, since the object is inside sphere S_k, all springs connected to the object must intersect the sphere (Fig. 3a), which violates the distribution condition. In order to realize the desired stiffness matrix, more complicated elastic components (screw springs) must be used.

Similarly, any simple serial mechanism with revolute joints enclosed by the sphere S_c associated with a given compliance matrix (as shown in Fig. 3b) cannot achieve the compliance regardless of the number of joints and the values of joint stiffnesses.

Another example of a serial mechanism that cannot achieve a given compliance matrix is illustrated in Fig. 3c. In this case, all joints are outside the sphere S_c associated with the compliance matrix and no axes of the joint twists intersect the sphere. For this case, the distances of the joint axes from the coordinate origin (the center of the sphere) are all greater than ρ_c. Thus, the mechanism cannot realize the compliance matrix even if helical joints are used.

C. Planar Case

The distribution conditions on elastic component geometry for the realization of a given elastic behavior are addressed in [28] for planar parallel mechanisms and in [29] for planar serial mechanisms. In planar elastic behavior realization, no screw springs or helical joints are used in these mechanisms. It can be seen that the distribution conditions of Propositions 1 and 2 apply to planar compliance realization as special cases.

For a 3×3 planar stiffness matrix $\mathbf{K}$, if $\mathbf{K}$ is partitioned in the form (4), then $\mathbf{A} \in \mathbb{R}^{2\times2}$, $\mathbf{B} \in \mathbb{R}^{2\times1}$ and $\mathbf{D} \in \mathbb{R}^{1\times1}$. The radius ρ_k can be determined by (32) and the corresponding S_k determined by (33) with $z = 0$, which is a circle in the plane. For the two eigenvalues of $\mathbf{A}$, the 2 cones symmetric to the two wrench-compliant axes (along the two eigenvectors) are represented by the two areas Λ_1 and Λ_2 bounded by 2 lines determined by the angle θ_1 and

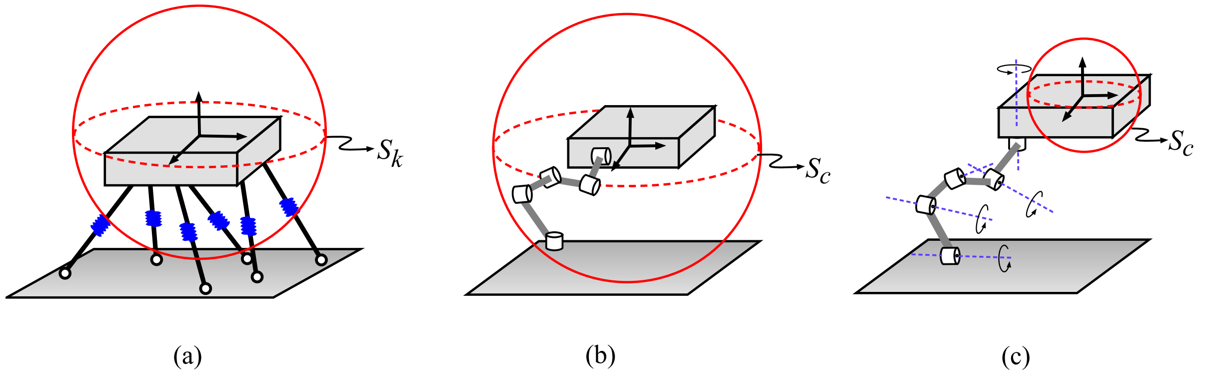

Fig. 3. Compliant behavior that cannot be achieved with a mechanism. (a) Realization of a stiffness matrix with a simple parallel mechanism: the suspended object is enclosed by sphere S_k. (b) Realization of a compliance matrix with a simple serial mechanism: all revolute joints are enclosed by sphere S_c. (c) Realization of a compliance matrix with a serial mechanism: no joint axes intersect sphere S_c.

θ_2 as shown in Fig. 4a. The distribution conditions on a planar parallel mechanism used to realize the stiffness matrix require that (i) at least one spring axis intersects circle S_k and at least one spring axis does not intersect the circle; and (ii) the spring position vectors $\mathbf{r}_i$s must be distributed in both areas Λ_1 and Λ_2 as illustrated in Fig. 4a.

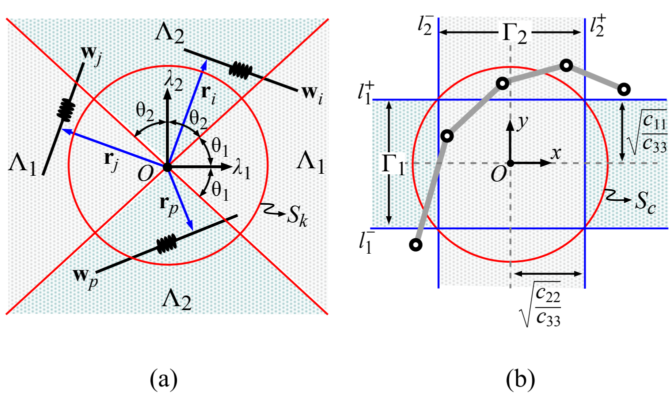

Fig. 4. Distribution of elastic components in planar mechanisms. (a) Parallel mechanism: at least one spring must intersect circle S_k and at least one spring must not intersect S_k; vectors $\mathbf{r}_i$s must be distributed in both areas Λ_1 and Λ_2. (b) Serial mechanism: at least one joint must be located inside circle S_c and at least one joint must be located outside S_c; at least one joint must be located within the area Γ_i and at least one joint must be located outside the area Γ_i $(i = 1, 2)$.

For a 3×3 planar compliance matrix $\mathbf{C}$, the sphere S_c becomes a circle of radius ρ_c in the plane. Since all joint axes in a planar serial mechanism are perpendicular to the plane, there is no constraint on the joint axis directions. Using a similar process [29], it can be shown that the joint location distribution is restricted by the two areas Γ_1 and Γ_2 bounded by two pairs of lines $l_1^{\pm}$ and $l_2^{\pm}$ parallel to the coordinate axes respectively. The two pairs of lines are defined by

$$l_1^{\pm} : y = \pm\sqrt{\frac{c_{11}}{c_{33}}}, \qquad l_2^{\pm} : x = \pm\sqrt{\frac{c_{22}}{c_{33}}}, \tag{69}$$

where c_{ii} are the diagonal entries of $\mathbf{C}$. The distribution conditions on a planar serial mechanism used to realize the compliance matrix require that (i) at least one joint must be located inside circle S_c and at least one joint must be located outside the circle; and (ii) the joint position vectors $\mathbf{r}_i$s must be distributed in both areas Γ_1 and Γ_2. At least one joint must be located within the area Γ_i and at least one joint must be located outside the area Γ_i as illustrated in Fig. 4b.

D. Application of the Distribution Theory

The distribution requirements presented in Section III are only necessary conditions. A mechanism satisfying those conditions does not ensure that a given compliance is realized with the mechanism. To realize a desired compliance, synthesis procedures such as those presented in [9]–[12], [14]–[16] could be used. These approaches, however, provide no or limited control over mechanism geometry. The use of the distribution theory in conjunction with the existing geometric construction-based synthesis procedures [22] would make the process more efficient. As shown in [22], the selection of elastic components early in the process is arbitrarily. The remaining components can be selected from an acceptable subspace constrained by previously selected components. As the number of selected components increases, the acceptable subspace shrinks dramatically. Thus, in the early steps of selecting elastic components, the distribution conditions need to be considered so that the remaining components can be selected from a larger available subspace, providing the opportunity for a more desirable mechanism geometry.

VI. Summary

In this paper, an easy to assess set of necessary conditions on the distribution of elastic components in a compliant mechanism used to realize an arbitrary compliance is identified. The physical significance of each condition is presented. This physical significance provides better understanding of and insight into general elastic behavior and its realization with either a fully parallel or a fully serial mechanism. In application, the distribution conditions can be used in existing compliance synthesis processes to more effectively select elastic components and to achieve a more desirable mechanism geometry.

References

[1] D. E. Whitney, "Quasi-static assembly of compliantly supported rigid parts," *ASME Journal of Dynamic Systems, Measurement, and Control*, vol. 104, no. 1, pp. 65–77, 1982.

[2] N. Hogan, "Impedance control: An approach to manipulation," *ASME Journal of Dynamic Systems, Measurements, and Control*, vol. 107, no. 1, pp. 1–7, 1985.

[3] F. M. Dimentberg, *The Screw Calculus and its Applications in Mechanics*. Foreign Technology Division, Wright-Patterson Air Force Base, Dayton, Ohio. Document No. FTD-HT-23-1632-67, 1965.

[4] R. S. Ball, *A Treatise on the Theory of Screws*. London, U.K.: Cambridge University Press, 1900.

[5] M. Griffis and J. Duffy, "Kinestatic control: A novel theory for simultaneously regulating force and displacement," *ASME Journal of Mechanical Design*, vol. 113, no. 4, pp. 508–515, 1991.

[6] T. Patterson and H. Lipkin, "Structure of robot compliance," *ASME Journal of Mechanical Design*, vol. 115, no. 3, pp. 576–580, 1993.

[7] J. Loncaric, "Normal forms of stiffness and compliance matrices," *IEEE Journal of Robotics and Automation*, vol. 3, no. 6, pp. 567–572, December 1987.

[8] M. Zefran and V. Kumar, "A geometrical approach to the study of the cartesian stiffness matrix," *ASME Journal of Mechanical Design*, vol. 124, no. 1, pp. 30–38, 2002.

[9] S. Huang and J. M. Schimmels, "The bounds and realization of spatial stiffnesses achieved with simple springs connected in parallel," *IEEE Transactions on Robotics and Automation*, vol. 14, no. 3, pp. 466–475, June 1998.

[10] R. G. Roberts, "Minimal realization of a spatial stiffness matrix with simple springs connected in parallel," *IEEE Transactions on Robotics and Automation*, vol. 15, no. 5, pp. 953–958, October 1999.

[11] S. Huang and J. M. Schimmels, "Achieving an arbitrary spatial stiffness with springs connected in parallel," *ASME Journal of Mechanical Design*, vol. 120, no. 4, pp. 520–526, December 1998.

[12] N. Ciblak and H. Lipkin, "Synthesis of cartesian stiffness for robotic applications," in *Proceedings of the IEEE International Conference on Robotics and Automation*, Detroit, MI, May 1999, pp. 2147–2152.

[13] S. Huang and J. M. Schimmels, "The eigenscrew decomposition of spatial stiffness matrices," *IEEE Transactions on Robotics and Automation*, vol. 16, no. 2, pp. 146–156, April 2000.

[14] S. Huang and J. M. Schimmels, "The duality in spatial stiffness and compliance as realized in parallel and serial elastic mechanisms," *ASME Journal of Dynamic Systems, Measurement, and Control*, vol. 124, no. 1, pp. 76–84, 2002.

[15] K. Choi, S. Jiang, and Z. Li, "Spatial stiffness realization with parallel springs using geometric parameters," *IEEE Transactions on Robotics and Automation*, vol. 18, no. 3, pp. 264–284, June 2002.

[16] M. B. Hong and Y. J. Choi, "Screw system approach to physical realization of stiffness matrix with arbitrary rank," *ASME Journal of Mechanisms and Robotics*, vol. 1, no. 2, pp. 021007(1–8), 2009.

[17] H. Su, D. Dorozhin, and J. Vance, "A screw theory approach for the conceptual design of flexible joints for compliant mechanisms," *ASME Journal of Mechanisms and Robotics*, vol. 1, no. 4, pp. 041 009(1–8), November 2009.

[18] J. Yu, S. Li, H. Su, and M. L. Culpepper, "Screw theory based methodology for the deterministic type synthesis of flexure mechanisms," *ASME Journal of Mechanisms and Robotics*, vol. 3, no. 3, pp. 031008(1–14), August 2011.

[19] G. Krishnan, C. Kim, and S. Kota, "A metric to evaluate and synthesize distributed compliant mechanisms," *ASME Journal of Mechanical Design*, vol. 135, no. 1, pp. 011004(1–9), January 2013.

[20] S. Kirmse, L. F. Campanile, and A. Hasse, "Synthesis of compliant mechanisms with selective compliance – An advanced procedure," *Mechanism and Machine Theory*, vol. 157, 104184, March 2021.

[21] S. Briot and W. Khalil, "Recursive and symbolic calculation of the elastodynamic model of flexible parallel robots," *International Journal of Robotic Research*, vol. 33, no. 3, pp. 469–483, 2014.

[22] S. Huang and J. M. Schimmels, "Geometric construction-based realization of spatial elastic behaviors in parallel and serial manipulators," *IEEE Transactions on Robotics*, vol. 34, no. 3, pp. 764–780, 2018.

[23] K. Wang, H. Dong, C. Qiu, I. Chen, and J. Dai, "Repelling-screw-based geometrical interpretation of dualities of compliant mechanisms," *Mechanism and Machine Theory*, vol. 169, 104636, March 2022.

[24] S. Huang and J. M. Schimmels, "The relationship between mechanism geometry and the centers of stiffness and compliance," *Mechanism and Machine Theory*, vol. 167, 104565, January 2022.

[25] R. G. Roberts and T. A. Shirey, "Synthesizing any specified elastic behavior with a hybrid connection of simple compliant components," in *Proceeding of the IEEE/RSJ International Conference on Intelligent Robots and Systems*, LasVegas, Nevada, USA, March 2003, pp. 3264–3269.

[26] M. B. Hong and Y. J. Choi, "Design method of planar three-degrees-of-freedom serial compliance device with desired compliance characteristics," *Journal of Mechanical Engineering Science*, vol. 226, no. 9, pp. 2331-2344, September 2012.

[27] S. Huang and J. M. Schimmels, "The bounds and realization of spatial compliances achieved with simple serial elastic mechanisms," *IEEE Transactions on Robotics and Automation*, vol. 16, no. 1, pp. 99–103, February 2000.

[28] S. Huang and J. M. Schimmels, "Planar compliance realization with two 3-joint serial manipulators connected in parallel," *ASME Journal of Mechanisms and Robotics*, vol. 14, no. 5, pp. 051007(1–12), October 2022.

[29] S. Huang and J. M. Schimmels, "Compliance realization with serial mechanisms having fixed link lengths," *ASME Journal of Mechanical Design*, vol. 144, no. 4, pp. 083301(1–12), August 2022.